Chinese Chemical Letters 31 (2020) 2503–2506

Contents lists available at ScienceDirect

Chinese Chemical Letters

journal homepage: www.elsevier.com/locate/cclet

Communication

Synthesis, structure and magnetic properties of a decanuclear Fe(III)/oxo cluster

Waseem Muhammad[a], Jie Ni[a], Zvonko Jagličić[d,**], Ping Cui[a,b,c,*], Linna Gao[e], Di Sun[a,f,*]

[a] School of Chemistry and Chemical Engineering, Key Lab of Colloid and Interface Chemistry, Ministry of Education, Shandong University, Ji'nan 250100, China
[b] Key Laboratory of Advanced Energy Materials Chemistry (Ministry of Education), College of Chemistry, Nankai University, Tianjin 300071, China
[c] College of Chemistry, Chemical Engineering and Materials Science, Shandong Provincial Key Laboratory of Clean Production of Fine Chemicals, Shandong Normal University, Ji'nan 250014, China
[d] Institute of Mathematics, Physics and Mechanics & Faculty of Civil and Geodetic Engineering, University of Ljubljana, Jadranska 19, Ljubljana, Slovenia
[e] College of Chemical and Environmental Engineering, Shandong University of Science and Technology, Qingdao 266590, China
[f] Shandong Provincial Key Laboratory of Chemical Energy Storage and Novel Cell Technology, and School of Chemistry and Chemical Engineering, Liaocheng University, Liaocheng 252000, China

ARTICLE INFO

Article history:
Received 14 October 2019
Received in revised form 5 January 2020
Accepted 13 January 2020
Available online 14 January 2020

Keywords:
Fe cluster
X-ray structure
Hydroxymethyl-pyrazole ligand
ESI-MS
Magnetic property

ABSTRACT

An iron (III) cluster, namely $[Fe_{10}(\mu_3\text{–}O)_8L_8(NO_3)_6]$ (**1**), has been synthesized by treatment of Fe $(NO_3)_3{\cdot}9H_2O$ with 3,5–dimethyl–1–(hydroxymethyl)–pyrazole (HL) under ambient temperature. The core skeleton of $\{Fe^{III}_{10}\}$ can be regarded as a pear-like cage with eight triangular $\{Fe^{III}_3(\mu_3\text{–}O)\}$ units, in which each three Fe^{III} centers is held together by one $\mu_3\text{–}O^{2-}$ group with Fe^{III} centers as corner-sharing triangle units. Importantly, $\{Fe^{III}_{10}\}$ cluster is not only stable in solid state but also in solution, which is confirmed by powder X-ray diffraction (PXRD) pattern and electrospray ionization mass spectrometry (ESI-MS), respectively. Furthermore, **1** shows antiferromagnetic exchange behavior arising from the interactions between the iron(III) centers.

There is a great interest in the investigation of polynuclear transition metal clusters due to their aesthetically pleasing structures and promising applications in the fields including magnetic materials, heterogeneous catalysis and optoelectronic nanodevices *etc*. [1–5]. Until now, a large number of metal clusters have been constructed spreading from alkaline metals [6], lanthanides [7] to late transition metals [8]. Consequently, many landmark clusters, such as $\{Ag_{490}\}$ [9], $\{Mo_{368}\}$ [10], $\{Fe_{168}\}$ [11], $\{Mn_{84}\}$ [12], $\{Co_{36}\}$ [13], $\{Ni_{34}\}$ [14] and $\{Gd_{140}\}$ [15], were accessed with the protection from suitable organic or/and inorganic ligands to avoid the aggregation of metal clusters. Our group principally focuses on assembly of metal clusters and their nucleation/assembly mechanisms were comprehensively investigated by using electrospray ionization mass spectrometry (ESI-MS). Some unprecedented examples such as $\{Ag_{180}\}$ [16], $\{Ag_{44}\}$ [17], $\{Ag_{48}\}$ [18], $\{Ag_{50}\}$ [17], $\{Ag_{52}\}$ [19], $\{Ag_{56}\}$ [20], $\{Ag_{76}\}$ [19] and $\{Ag_{211}\}$ [21] have been synthesized and fully characterized.

Encouraged by these preliminary works, we turned our attention to the ferric clusters since earth abundant storage of iron elements and fascinating chemical and physical properties of these clusters. Construction of polynuclear iron clusters is of paramount important not only for fundamental studies in bioinorganic chemistry [22], but also their potential utility as molecular magnetic materials [23]. Indeed, hundreds of proteins host iron-sulfur clusters and iron oxides/hydroxides exist extensively in several biological systems including nonheme metalloproteins [24] and iron storage protein ferritin [25]. Additionally, although the interaction between iron(III) centers is predominantly antiferromagnetic, the appreciable magnetic anisotropy along with high ground-state spin and even single-molecule-magnet behavior have also been found in high-nuclear iron clusters. To our surprise, only a few homonuclear iron clusters have been reported, such as $\{Fe^{III}_4\}$ [26], $\{Fe^{III}_8\}$ [27], $\{Fe^{III}_{10}\}$ [28]. However, rational design and assemble high-nuclear iron clusters, especially the core topology adjustment is still a great challenging, thus hindering progress in this area.

Recently, we have reported novel brucite-disc $\{Mn^{II}_{15}Mn^{III}_4\}$ [29] cluster, core-shell heterometallic disc-like $\{Mn_7\subset(Mn,Cd)_{12}\}$

* Corresponding authors at: School of Chemistry and Chemical Engineering, Key Lab of Colloid and Interface Chemistry, Ministry of Education, Shandong University, Ji'nan 250100, China.
** Corresponding author.
E-mail addresses: zvonko.jaglicic@imfm.si (Z. Jagličić), cuiping@sdu.edu.cn (P. Cui), dsun@sdu.edu.cn (D. Sun).

https://doi.org/10.1016/j.cclet.2020.01.031
1001-8417/

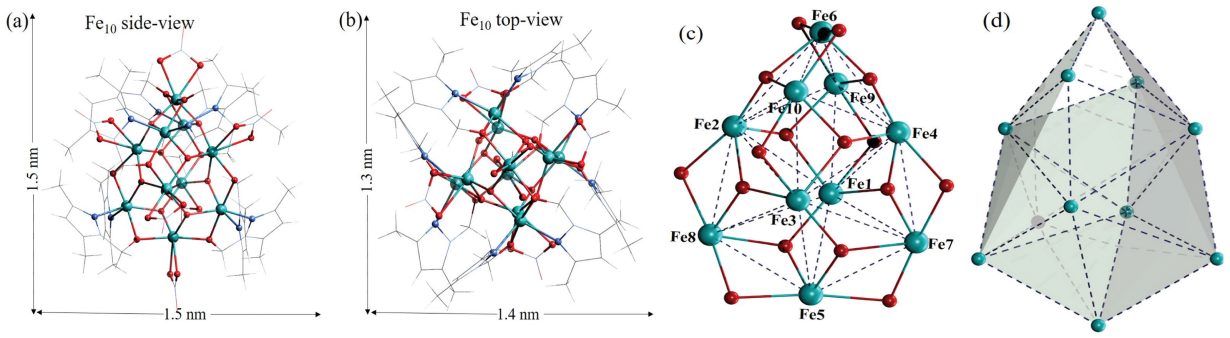

Fig. 1. (a, b) The molecular structure of **1** viewed along two different views. All uncoordinated atoms are shown using the wireframe style for clarity. (c) The $\{Fe^{III}_{10}(\mu_3\text{–}O)_8(\mu_2\text{–}O)_8\}$ core with eight triangular $\{Fe^{III}_3(\mu_3\text{–}O)\}$ units, in which all the μ_2–O groups come from the L^- ligands. (d) The pear-like $\{Fe^{III}_{10}\}$ cage. The dashed lines binding the metal ions are to description the shape of the $\{Fe^{III}_{10}\}$ metallic skeleton. Color scheme: Fe, skyblue; O, red; N, blue; C, gray; H, white.

[30] cluster, cubane-like octanuclear $\{Mn^{III}_2Mn^{II}_6\}$ [31] cluster, and bicubane-like tetranuclear $\{Co^{II}_4\}$ [32] cluster supported by bidentate hydroxymethyl-pyrazole ligands, which are capable of stabilizing different metal clusters with different coordination modes. Inspired by these results, we were interested in the reactions of iron salts with hydroxymethyl-pyrazole ligands to confirm the corresponding structures and magnetic properties. Herein, we report the synthesis, structural characterization, and magnetic properties of a decanuclear Fe(III)/oxo cluster, which was isolated as $[Fe_{10}(\mu_3\text{–}O)_8L_8(NO_3)_6]$ (**1**). Moreover, we employed ESI-MS to investigate its behavior in solution.

Crystallographic analysis reveals that **1** crystallizes in the triclinic space group *P*–1 and crystallographic data are detailed in Tables S1 and S2 (Supporting information). The most intriguing feature of **1** is that the asymmetric unit consists of one $[Fe_{10}(\mu_3\text{–}O)_8L_8(NO_3)_6]$ nanocluster (1.3 × 1.4 nm) with eight peripheral L^- ligands coating the $\{Fe_{10}(\mu_3\text{–}O)_8\}$ core surrounded by additional six bidentate chelating NO_3^- anions (Figs. 1a and b). The metallic skeleton of $\{Fe_{10}\}$ core can be described as a pear-like cage with eight triangular $\{Fe_3(\mu_3\text{–}O)\}$ units (Figs. 1c and d). Each three Fe centers is held together by one μ_3–O group acting as corner-sharing triangle units. This $\{Fe_3O\}$ triangle is common in iron-oxo chemistry and has acted as a building block for many higher nuclearity clusters [33]. The oxidation states of the Fe atoms and the protonation levels of O atoms were assigned on the basis of bond valence sum (BVS) calculations (Table S3 in Supporting information), charge considerations and inspection of interatomic distances (Fe–O and Fe–N) [33]. The results clearly indicated that all metal ions correspond to Fe(III) (BVS 2.972–3.153), and the oxygen valence state of μ_3–O is -2. All Fe^{3+} ions are exclusively six-coordinated in distorted octahedral geometries, displaying two different coordination environments (FeO6 for Fe1–6 and FeO4N2 for Fe7–10). The six O atoms around Fe1–6 centers come from μ_3–O groups, NO_3– anions and hydroxyl groups attached to L^- ligands. Coordination geometries about Fe1–4 centers are completed by three μ_3–O groups, one bidentate chelating NO_3^- anion and one L^- ligand. At the periphery of Fe5 and Fe6 centers, the O atoms are from two μ_3–O groups, one bidentate chelating NO_3^- anion and two L^- ligands. Compared with Fe1–6 centers, Fe7–10 centers are surrounded by an O4N2 donor set, which is analogous to those of Fe5 and Fe6 centers except that one chelating NO_3^- anion is replaced by two N atoms from two unique L^- ligands. The Fe—O and Fe—N bond lengths are in the normal ranges of 1.891(5)-2.336 (5) Å and 2.121(7)-2.187(7) Å, respectively.

Moreover, all L^- ligands adopt the same $\mu_2\text{-}\eta_N{}^1\text{:}\eta_O{}^2$ bonding mode to connect two metal centers of the triangle unit(Fig. 1a), which further consolidate the stability of the $\{Fe_{10}(\mu_3\text{–}O)_8\}$ core. Such coordination mode is commonly observed in L^- based polynuclear complexes [29,30,34]. Notably, eight such bulky ligands at the exterior of the $\{Fe_{10}(\mu_3\text{–}O)_8\}$ core fully protect the core, thus restricting the further growth. The shortest Fe···Fe distance between two adjacent $[Fe_{10}(\mu_3\text{-}O)_8L_8(NO_3)_6]$ molecules is between Fe5 and Fe8 at 7.801 Å (Fig. S1 in Supporting information).

To check the phase purity of **1**, powder X-ray diffraction (PXRD) pattern of the bulk sample was measured. The main peaks are primarily in agreement with the pattern simulated from single-crystal X-ray diffraction data, suggesting the phase purity of the as-synthesized sample (Fig. S2 in Supporting information). The slight difference between the simulated and experimental patterns may be caused by the different orientation of the crystals in the bulk powder sample. Thermogravimetic analysis (TGA) of **1** was carried out from room temperature to 800 °C under nitrogen atmosphere (Fig. S3 in Supporting information). There was no obvious weight loss before 250 °C, after which the framework structure began to collapse upon further heating. Furthermore, the solid-state optical diffuse reflectance spectrum of **1** was studied at room temperature. As shown in Fig. 2, the absorption spectrum of **1** shows one main peak centered at 350 nm and a wide low-energy peak from 450 nm to 540 nm in the UV–vis region, which should be assigned to $\pi\rightarrow\pi^*$ electron transition on ligand and charge transfer between ligand and metal ion. Meanwhile, the band gap of **1** was estimated to be 1.43 eV from its Tauc plot of $(Ahv)^{1/2}$ *versus hv*, in agreement with the color of **1**. The result revealed that **1** shows better light-harvesting ability.

To investigate its solution behavior of the cluster, the ESI-MS of **1** dissolved in dichloromethane was performed in positive-ion model. As shown in Fig. 3, three identifiable species (**1a**–**1c**) with the charge state of +1 are observed in the *m*/*z* range of 1900–2300. The measured mass spectra well match the calculated isotopic distribution patterns. Their assigned formulae are given in the

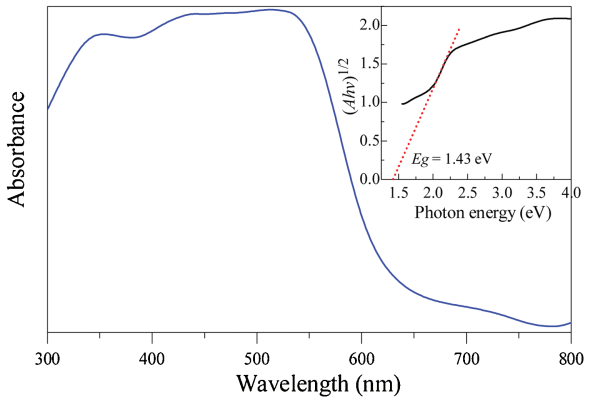

Fig. 2. UV–vis spectrum of **1** in the solid state. Inset: Tauc plot of **1**.

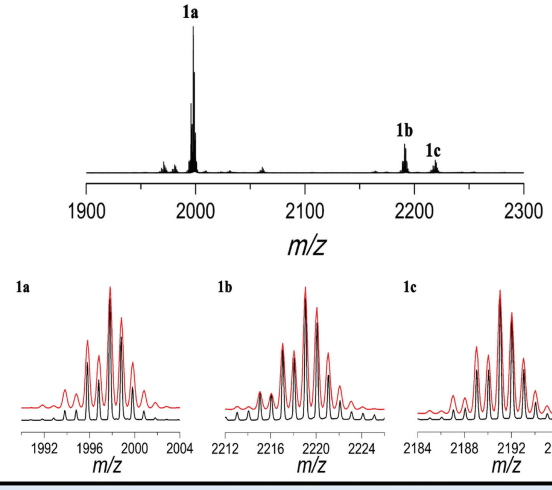

Peak	Species	Exp. *m/z*	Cal. *m/z*
1a	$[Fe_{10}O_8L_8(NO_3)_5]$	1997.80	1997.82
1b	$[Fe_{10}O_8L_8(NO_3)_4(C_2H_5OH)_3(H_2O)(CH_3CN)_2(OH)]$	2191.05	2191.02
1c	$[Fe_{10}O_8L_8(NO_3)_4(C_2H_5OH)_4(CH_3CN)_2(OH)]$	2219.08	2219.05

Fig. 3. Positive–ion mode ESI–MS spectrum of **1** dissolved in dichloromethane and comparison of the experimental (black) and calculated (red) isotopic envelopes for **1a**–**1c**. Detailed formulae of each species are given in the table.

table in Fig. 3. The predominant species **1a** centered at m/z = 1997.80 corresponds to $[Fe_{10}O_8L_8(NO_3)_5]^+$ (calcd. 1997.82), which is formed by losing one NO_3^- ion from the parent cluster. The species **1b** centered at m/z = 2191.05 can be assigned to a species $[Fe_{10}O_8L_8(NO_3)_4(C_2H_5OH)_3(H_2O)(CH_3CN)_2(OH)]^+$ (calcd. 2191.02) resulting from ligand exchange between NO_3^- and OH^-. Additionally, we find that species **1c** located at m/z = 2219.08 can be attributed to a species $[Fe_{10}O_8L_8(NO_3)_4(C_2H_5OH)_4(CH_3CN)_2(OH)]^+$ (calcd. 2219.05), which is generated from **1b** through some solvent exchange. Compared to the crytstallographic result of **1**, all these species contain cores of $[Fe_{10}O_8L_8(NO_3)_n]$ ($n_{\mathbf{1a-1c}}$ = 5, 4, 4), which clearly illustrate the stability of Fe_{10} cluster in solution.

The direct current (dc) magnetic susceptibility measurement on sample of **1** was performed in the temperature range of 2–300 K at an applied magnetic field of 1 kOe. As shown in Fig. 4a, the susceptibility χ_M increases with decreasing temperature until at T_{max} =18 K it reaches a maximal value of 0.077 emu/mol. The observed broad maximum of susceptibility is a clear indication of prevailing antiferromagnetic interaction between the ten magnetic moments of Fe^{3+} ions in a molecule. The product $\chi \cdot T$ at room temperature is 13.6 emu K/mol (Fig. S4 in Supporting information). This value is much smaller in comparison to the expected value for ten non-interacting Fe^{3+} ions (S = 5/2, g = 2.0) per molecule that is 43.5 emu K/mol. We used the relation $(\chi \cdot T)_{expected} = 10 \cdot \mu^2_{eff}/8$ [35] and $\mu_{eff} = 5.9\ \mu_B$ for Fe^{3+} ion [36]. The small value of the product $\chi \cdot T$ at room temperature means that already at room temperature there are rather large antiferromagnetic interactions between magnetic moments in a molecule. Similar phenomenon has been observed in previously reported Fe-containing clusters [37,38]. The same conclusion can be obtained from the temperature dependent inverse susceptibility (Fig. 4b) that is non-linear in the whole investigated temperature range. This means that **1** does not behave like a paramagnet even at room temperature. Finally, the isothermal magnetization at 10 K (Fig. 4c) is linear up to the maximal magnetic field of 50 kOe with very small value of the magnetization of 0.043 μ_B per Fe^{3+} ion in the field of 50 kOe. For non-interacting Fe^{3+} ions one would expect $\approx 5\ \mu_B$ per Fe^{3+} ion in saturation [36]. All these experimental data are in agreement with rather large antiferromagnetic interaction between ten Fe^{3+} magnetic moments in a molecule of **1**.

A theoretical consideration of the magnetic interactions between Fe^{3+} ions with spin $S = 5/2$ would require a solving an interaction Hamiltonian. With ten ions in a molecule where, taking into account the comparable distances between them, each magnetic moment interacts with more than two neighbors, solving of such a Hamiltonian would be formidable task and exceeds our computational possibilities and purpose of this paper. Still, some qualitative analysis of the measured data can be made.

Note that the non-linear $\chi_M^{-1}(T)$ dependence prevents us from direct determination of the Curie-Weiss temperature θ. However, the curve of $\chi_M^{-1}(T)$ shows that the tangent at arbitrary temperature above 50 K would cross the temperature axis at a large negative value of the order of several hundred K. Such a large Curie-Weiss temperature θ, which means considerable antiferromagnetic interactions, is in agreement with the small susceptibility measured already at the room temperature. On the other hand, it is worth to note on a big discrepancy between the large negative θ and the T_{max} at a rather low temperature of 18 K. Ramirez [39] has introduced an empirical factor $f = |\theta|/T_{max}$ that compares the Curie-Weiss temperature and the critical temperature of magnetic ordering. In our case the factor f is larger than 10. Such a large value is characteristic for magnetically frustrated systems. According to the structure of **1** it is not surprising. Ten Fe(III) ions in a molecule are composing many triangles with Fe(III) ions in their corners and similar distances between them (*i.e.*, Fe1–Fe2–Fe9, Fe2–Fe3–Fe8, ···). Together with the antiferromagnetic interactions between these magnetic moments, the **1** may belong to a geometrically frustrated systems [40].

In summary, a new decanuclear Fe(III)/oxo cluster has been successfully prepared by reaction of iron(III) salt and 3,5–dimethyl–1–(hydroxymethyl)–pyrazole ligand under basic condition at room temperature, which contains pear-like $\{Fe_{10}(\mu_3\text{–}O)_8\}$

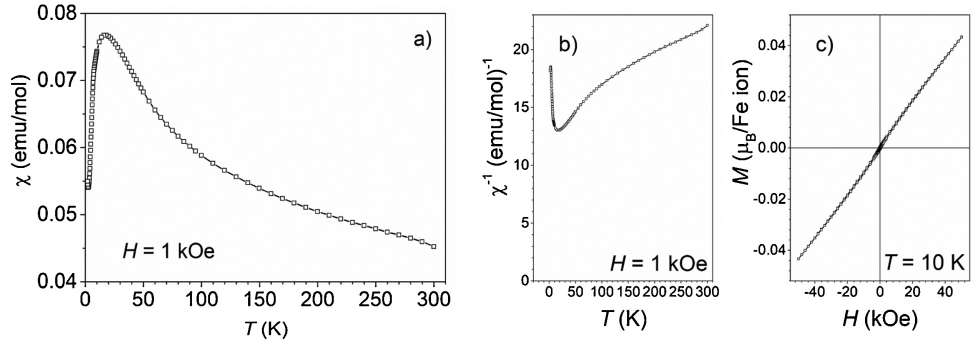

Fig. 4. (a) Temperature dependence of the magnetic susceptibility (χ_M). (b) inverse susceptibility (χ_M^{-1}) of **1**. (c) Isothermal magnetization curve at 10 K of **1**.

core protected by eight bidentate hydroxymethyl-pyrazole ligands and six NO_3^- ions. The formation of this novel cluster {Fe_{10}} in solution was also monitored by ESI-MS, which is indicative of its stability in dichloromethane and its ligand exchange behavior in solvents. Magnetic measurements indicate the possibly antiferromagnetic interaction between the Fe(III) centers. The successful fabrication of **1** not only expands the types of polynuclear metal clusters supported by bidentate hydroxymethyl-pyrazole ligand but also provides a promising approach to construct polynuclear iron clusters with stability in solution. Development of other functional polynuclear compounds with improved optical and magnetic properties is currently in progress in our laboratory.

Declaration of competing interest

The authors declare that they have no known competing financial interests or personal relationships that could have appeared to influence the work reported in this paper.

Acknowledgments

We gratefully acknowledge financial support from the National Natural Science Foundation of China (Nos. 21071188, 91961105, 21822107, 21571115 and 21827801), the Natural Science Foundation of Shandong Province (Nos. ZR2019ZD45, JQ201803 and ZR2017MB005), the Key R&D Program of Shandong Province (No. 2019GSF108158), Shandong Provincial Key Laboratory of Clean Production of Fine Chemicals (No. 2019FCCEKL06), the Taishan Scholar Project of Shandong Province of China (Nos. tsqn201812003 and ts20190908), the Fundamental Research Funds of Shandong University (No. 2018JC046), and the Slovenian Research Agency (No. P2-0348).

Appendix A. Supplementary data

Supplementary material related to this article can be found, in the online version, at doi:https://doi.org/10.1016/j.cclet.2020.01.031.

References

[1] Y.Z. Zheng, G.J. Zhou, Z.P. Zheng, et al., Chem. Soc. Rev. 43 (2014) 1462–1475.
[2] P. Buchwalter, J. Rosé, P. Braunstein, Chem. Rev. 115 (2015) 28–126.
[3] Q.M. Wang, Y.M. Lin, K.G. Liu, Acc. Chem. Res. 48 (2015) 1570–1579.
[4] R.W. Huang, Y.S. Wei, X.Y. Dong, et al., Nat. Chem. 9 (2017) 689–697.
[5] J.B. Peng, Q.C. Zhang, X.J. Kong, et al., Angew. Chem. Int. Ed. 50 (2011) 10649–10652.
[6] M. Arrowsmith, M.S. Hill, D.J. MacDougall, et al., Angew. Chem. Int. Ed. 48 (2009) 4013–4016.
[7] J. Dong, P. Cui, P.F. Shi, et al., J. Am. Chem. Soc. 137 (2015) 15988–15991.
[8] T. Sawada, M. Yoshizawa, S. Sato, et al., Nat. Chem. Biol. 1 (2009) 53–56.
[9] C.E. Anson, A. Eichhöfer, I. Issac, et al., Angew. Chem. Int. Ed. 47 (2008) 1326–1331.
[10] A. Müller, E. Beckmann, H. Bögge, et al., Angew. Chem. Int. Ed. 41 (2002) 1162–1167.
[11] Z.M. Zhang, S. Yao, Y.G. Li, et al., J. Am. Chem. Soc. 131 (2009) 14600–14601.
[12] A.J. Tasiopoulos, A. Vinslava, W. Wernsdorfer, et al., Angew. Chem. Int. Ed. 43 (2004) 2117–2121.
[13] P. Alborés, E. Rentschler, Angew. Chem. Int. Ed. 48 (2009) 9366–9370.
[14] D. Fenske, J. Ohmer, J. Hachgenei, Angew. Chem. Int. Ed. 24 (1985) 993–995.
[15] X.Y. Zheng, Y.H. Jiang, G.L. Zhuang, et al., J. Am. Chem. Soc. 139 (2017) 18178–18181.
[16] Z. Wang, H.F. Su, Y.Z. Tan, et al., Proc. Natl. Acad. Sci. U. S. A. 114 (2017) 12132–12137.
[17] Z. Wang, H.F. Su, C.H. Tung, et al., Nat. Commun. 9 (2018) 4407.
[18] S.S. Zhang, F. Alkan, H.F. Su, et al., J. Am. Chem. Soc. 141 (2019) 4460–4467.
[19] J.W. Liu, L. Feng, H.F. Su, et al., J. Am. Chem. Soc. 140 (2018) 1600–1603.
[20] Z. Wang, H.F. Su, M. Kurmoo, et al., Nat. Commun. 9 (2018) 2094.
[21] J.Y. Liu, F. Alkan, Z. Wang, et al., Angew. Chem. Int. Ed. 58 (2019) 195–199.
[22] K.L. Taft, G.C. Papaefthymiou, S.J. Lippard, Science 259 (1993) 1302–1305.
[23] L.F. Jones, E.K. Brechin, D. Collison, et al., Inorg. Chem. 42 (2003) 6601–6603.
[24] E.C. Theil, Ann. Rev. Biochem. 56 (1987) 289–315.
[25] E.C. Theil, M. Matzapetakis, X. Liu, JBIC, J. Biol. Inorg. Chem. 11 (2006) 803–810.
[26] A.L. Barra, A. Caneschi, A. Cornia, et al., J. Am. Chem. Soc. 121 (1999) 5302–5310.
[27] D. Gatteschi, R. Sessoli, Angew. Chem. Int. Ed. 42 (2003) 268–297.
[28] C. Benelli, J. Cano, Y. Journaux, et al., Inorg. Chem. 40 (2001) 188–189.
[29] Y.K. Deng, H.F. Su, J.H. Xu, et al., J. Am. Chem. Soc. 138 (2016) 1328–1334.
[30] L.Y. Guo, H.F. Su, M. Kurmoo, et al., J. Am. Chem. Soc. 139 (2017) 14033–14036.
[31] W.F. Xie, L.Y. Guo, J.H. Xu, et al., Eur. J. Inorg. Chem. 20 (2016) 3253–3261.
[32] F. Yang, Y.K. Deng, L.Yu Guo, et al., CrystEngComm 18 (2016) 1329–1336.
[33] T. Taguchi, M.S. Thompson, K.A. Abboud, et al., Dalton Trans. 39 (2010) 9131–9139.
[34] I. Banerjee, M. Dolai, A.D. Jana, et al., CrystEngComm 14 (2012) 4972–4975.
[35] F.E. Mabbs, D.J. Machin, Magnetism and Transition Metal Complexes, Dover Publications, Inc., Mineola, New York, 1973.
[36] N.W. Ashcroft, N.D. Mermin, Solid State Physics, Saunders College Publishing, Fort Worth, 1976.
[37] S. Khanra, M. Helliwell, F. Tuna, et al., Dalton Trans. (2009) 6166–6174.
[38] H.C. Yao, Y.Z. Li, L.M. Zheng, et al., Inorg. Chim. Acta Rev. 358 (2005) 2523–2529.
[39] A.P. Ramirez, Annu. Rev. Mater. Sci. 24 (1994) 453–480.
[40] M. Pregelj, A. Zorko, O. Zaharko, et al., Phys. Rev. B 88 (2013) 224421.